1
Colloid Aspects of Cosmetic Formulations with Particular Reference to Polymeric Surfactants

Tharwat F. Tadros

Abstract

The use of polymeric surfactants for the stabilization of cosmetic and personal care formulations is described in terms of their adsorption and conformation at the solid/liquid and liquid/liquid interface. The most effective polymeric surfactants are the A–B, A–B–A block and BA_n or AB_n graft types (where B is the anchor chain and A is the stabilizing chain). The mechanism by which these polymeric surfactants stabiles suspensions and emulsions is briefly discussed in terms of their interaction when particles or droplets approach. This provides very strong repulsion, which is referred to as steric stabilization. Particular attention is given to a recently developed graft copolymer AB_n based on inulin (which is extracted from chicory roots) that is hydrophobized by grafting several alkyl groups (B) onto the linear polyfructose chain (A). This polymeric surfactant is referred to as hydrophobically modified inulin (HMI) and is commercially available as INUTEC® SP1 (ORAFTI, Belgium). It is used for the stabilization of oil-in-water (O/W) emulsions both in aqueous media and in the presence of high electrolyte concentrations. The emulsions remained stable for more than one year at room temperature and at 50 °C. INUTEC® SP1 is also effective in reducing Ostwald ripening in nano-emulsions. It could also be applied for the preparation of W/O/W and O/W/O multiple emulsions and for stabilization of liposomes and vesicles. Based on these fundamental studies, INUTEC® SP1 could be applied for the preparation of stable personal care formulations. The amount of polymeric surfactant required for maintenance of stability (for more than one year at ambient temperature) was relatively low (of the order of 1 w/w% based on the oil phase). In addition, the polymeric surfactant showed no skin irritation, no stickiness or greasiness and it gave an excellent skin-feel.

For the optimum formulation of cosmetic preparations, colloid and interface principles have to be applied. The most effective stabilizers against flocculation and coalescence are polymeric surfactants of the A–B, A–B–A block and BA_n or AB_n graft types (where B is the anchor chain and A is the stabilizing chain).

Colloids and Interface Science Series, Vol. 4
Colloids in Cosmetics and Personal Care. Edited by Tharwat F. Tadros

ISBN: 978-3-527-31464-5

Polymeric surfactants also reduce Ostwald ripening in nano-emulsions. They are also applied for the stabilization of multiple emulsions of both the W/O/W and the O/W/O types. Polymeric surfactants are also used for stabilization of liposomes and vesicles. These benefits of polymeric surfactants justify their application in cosmetic and personal care preparations. Apart from their excellent stabilization effect, they can also eliminate any skin irritation.

1.1 Introduction

Cosmetic and toiletry products are generally designed to deliver a function benefit and to enhance the psychological well-being of consumers by increasing their esthetic appeal. Thus, many cosmetic formulations are used to clean hair, skin, etc., and impart a pleasant odor, make the skin feel smooth and provide moisturizing agents, provide protection against sunburn, etc. In many cases, cosmetic formulations are designed to provide a protective, occlusive surface layer, which either prevents the penetration of unwanted foreign matter or moderates the loss of water from the skin [1, 2]. In order to have consumer appeal, cosmetic formulations must meet stringent esthetic standards such as texture, consistency, pleasing color and fragrance and convenience of application. This results in most cases in complex systems consisting of several components of oil, water, surfactants, coloring agents, fragrants, preservatives, vitamins, etc. In recent years, there has been considerable effort in introducing novel cosmetic formulations that provide great beneficial effects to the customer, such as sunscreens, liposomes and other ingredients that may maintain healthy skin and provide protection against drying, irritation, etc.

Since cosmetic products come into close contact with various organs and tissues of the human body, a most important consideration for choosing ingredients to be used in these formulations is their medical safety. Many of the cosmetic preparations are left on the skin after application for indefinite periods and, therefore, the ingredients used must not cause any allergy, sensitization or irritation. The ingredients used must be free of any impurities that have toxic effects.

One of the main areas of interest of cosmetic formulations is their interaction with the skin [3]. The top layer of the skin, which is the man barrier to water loss, is the stratum corneum, which protects the body from chemical and biological attack [4]. This layer is very thin, approximately 30 μm, consists of ~10% by weight of lipids that are organized in bilayer structures (liquid crystalline), and at high water content is soft and transparent. A schematic representation of the layered structure of the stratum corneum, suggested by Elias et al. [5], is given in Figure 1.1. In this picture, ceramides were considered as the structure-forming elements, but later work by Friberg and Osborne [6] showed the fatty acids to be the essential compounds for the layered structure and that a considerable part of the lipids are located in the space between the methyl groups. When a cosmetic formulation is applied to the skin, it will interact with the stratum corneum and

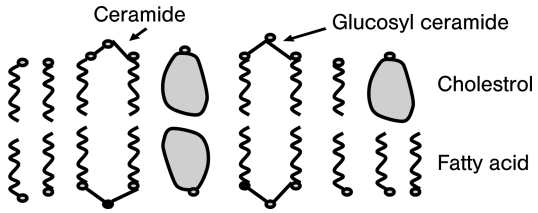

Figure 1.1 Schematic representation of the ''bilayer'' structure of the stratum corneum.

it is essential to maintain the ''liquid-like'' nature of the bilayers and prevent any crystallization of the lipids. This happens when the water content is reduced below a certain level. This crystallization has a drastic effect on the appearance and smoothness of the skin (''dry'' skin feeling).

To achieve the above criteria, ''complex'' multiphase systems are formulated: (1) oil-in-water (O/W) emulsions; (2) water-in-oil (W/O) emulsions; (3) solid/liquid dispersions (suspensions); (4) emulsion–suspension mixtures (suspoemulsions); (5) nanoemulsions; (6) nanosuspensions; (7) multiple emulsions. All these disperse systems contain ''self-assembly'' structures: (1) micelles (spherical, rod-shaped, lamellar); (2) liquid crystalline phases (hexagonal, cubic or lamellar); (3) liposomes (multilamellar bilayers) or vesicles (single bilayers). They also contain ''thickeners'' (polymers or particulate dispersions) to control their rheology.

The above complex multiphase systems require a fundamental understanding of the colloidal interactions between the various components. Understanding these interactions enables the formulation scientist to arrive at the optimum composition for a particular application. The fundamental principles involved also help in predicting the long-term physical stability of the formulations. Below a summary of some of the most commonly used formulations in cosmetics is given [7].

1. *Lotions:* These are usually (O/W emulsions that are formulated in such a way (see below the section on cosmetic emulsions) as to give a shear thinning system. The emulsion will have a high viscosity at low shear rates ($0.1\ s^{-1}$) in the region of few hundred Pa s, but the viscosity decreases very rapidly with increase in shear rate, reaching values of a few Pa s at shear rates greater than $1\ s^{-1}$.
2. *Hand creams:* These are formulated as O/W or W/O emulsions with special surfactant systems and/or thickeners to give a viscosity profile similar to that of lotions, but with orders of magnitude greater viscosities. The viscosity at low shear rates ($<0.1\ s^{-1}$) can reach thousands of Pa s and they retain a relatively high viscosity at high shear rates (of the order of few hundred Pa s at shear rates $>1\ s^{-1}$). These systems are sometimes described to have a ''body'' mostly in the form of a gel-network structure that may be achieved by the use of surfactant mixtures to form liquid crystalline structures. In some case, thickeners (hydrocolloids) are added to enhance the gel network structure.

3. *Lipsticks:* These are suspensions of pigments in a molten vehicle. Surfactants are also used in their formulation. The product should show good thermal stability during storage and rheologically it should behave as a viscoelastic solid. In other words, the lipstick should show small deformation at low stresses and this deformation should recover on removal of the stress. Such information could be obtained using creep measurements.
4. *Nail polishes:* These are pigment suspensions in a volatile non-aqueous solvent. The system should be thixotropic. On application by the brush it should show proper flow for an even coating but should have sufficient viscosity to avoid ''dripping''. After application, ''gelling'' should occur on a controlled time scale. If ''gelling'' is too fast, the coating may leave ''brush marks'' (uneven coating). If ''gelling'' is too slow, the nail polish may drip. The relaxation time of the thixotropic system should be accurately controlled to ensure good leveling, and this requires the use of surfactants.
5. *Shampoos:* These are normally a ''gelled'' surfactant solution of well-defined associated structures, e.g. rod-shaped micelles. A thickener such as a polysaccharide may be added to increase the relaxation time of the system. The interaction between the surfactants and polymers is of great importance.
6. *Antiperspirants:* These are suspensions of solid actives in a surfactant vehicle. Other ingredients such as polymers that provide good skin feel are added. The rheology of the system should be controlled to avoid particle sedimentation. This is achieved by addition of thickeners. Shear thinning of the final product is essential to ensure good spreadability. In stick application, a ''semi-solid'' system is produced.
7. *Foundations:* These are complex systems consisting of a suspension–emulsion system (sometimes referred to as suspoemulsions). Pigment particles are usually dispersed in the continuous phase of an O/W or W/O emulsion. Volatile oils such as cyclomethicone are usually used. The system should be thixotropic to ensure uniformity of the film and good leveling.

The overview in this chapter, which is by no means exhaustive, will deal with the following topics: (1) interaction forces between particles or droplets in a dispersion and their combination; (2) description of stability in terms of the interaction forces; (3) self-assembly structures and their role in stabilization, skin feel, moisturization and delivery of actives; and (4) use of polymeric surfactants for stabilization of nanoemulsions, multiple emulsions, liposomes and vesicles.

1.2 Interaction Forces and Their Combination

Three main interaction forces can be distinguished: (1) van der Waals attraction; (2) double layer repulsion; and (3) steric interaction. These interaction forces and their combination are briefly described below [8].

The van der Waals attraction is mainly due to the London dispersion forces, which arise from charge fluctuations in the atoms or molecules. For an assembly of atoms or molecules (particles or droplets), the attractive forces can be summed, resulting in long-range attraction. The attractive force or energy for two particles or droplets increases with decrease in separation distance between them and at short distances it reaches very high values. In the absence of any repulsive force, the particles or droplets in a dispersion will aggregate, forming strong flocs that cannot be redispersed by shaking.

The van der Waals attraction between two spherical particles or droplets each of radius R separated by a surface-to-surface distance of separation h, is given by the following expression (when $h \ll R$):

$$V_A = -\frac{AR}{12h} \tag{1}$$

where A is the effective Hamaker constant, given by

$$A = (A_{11}{}^{1/2} - A_{22}{}^{1/2})^2 \tag{2}$$

where A_{11} and A_{22} are the Hamaker constants of particles or droplets and medium, respectively.

The Hamaker constant A of any material is given by

$$A = \pi q^2 \beta \tag{3}$$

where q is the number of atoms or molecules per unit volume and β is the London dispersion constant (that is related to the polarizability of the atoms or molecules).

To counteract this attraction, one needs a repulsive force that operates at intermediate distances of separation between the particles. With particles or droplets containing a charge repulsion occurs as a result of formation of electrical double layers [9]. Repulsion results from charge separation and formation of electrical double layers, e.g. when using ionic surfactants. At low electrolyte concentrations ($<10^{-2}$ mol dm^{-3} NaCl) the double layers extend to several nanometers in solution. When two particles or droplets approach a distance of separation that becomes smaller than twice the double-layer extension, double-layer overlap occurs, resulting in strong repulsion. The repulsive force V_{el} is given by the following expression [10]:

$$V_{el} = \frac{4\pi\varepsilon_r\varepsilon_0 R^2 \psi_0{}^2 \exp(-\kappa h)}{2R + h} \tag{4}$$

where ε_r is the relative permittivity (78.6 for water at 25 °C), ε_0 is the permittivity of free space, R is the particle or droplet radius, ψ_0 is the surface potential (that is

approximately equal to the measurable zeta potential) and κ is the Debye–Hückel parameter that is related to the number of ions n_0 per unit volume (of each type present in solution) and the valency of the ions Z_i (note that $1/\kappa$ is a measure of the double-layer extension and is referred to as the "thickness of the double layer"):

$$\frac{1}{\kappa} = \left(\frac{\varepsilon_r \varepsilon_0 kT}{2n_0 {Z_i}^2 e^2}\right)^{1/2} \tag{5}$$

where k is Boltzmann's constant and T is the absolute temperature.

The magnitude of repulsion increases with increase in zeta potential and decrease in electrolyte concentration and decrease in valency of the counter and co-ions.

A more effective repulsion is due to the presence of adsorbed nonionic surfactants or polymers [11, 12]. These molecules consist of hydrophobic chains which adsorb strongly on hydrophobic particles or oil droplets and hydrophilic chains which are strongly solvated by the molecules of the medium. One can establish a thickness for the solvated (hydrated) chain. When two particles or droplets approach a distance of separation that is smaller than twice the adsorbed layer thickness, repulsion occurs as a result of two main effects: (1) unfavorable mixing of the solvated chains, which results in an increase in the osmotic pressure in the overlap region (solvent molecules diffuse, separating the particles or droplets), and is referred to as the mixing interaction, G_{mix}; and (2) a reduction in configurational entropy of the chains on significant overlap, which is referred to as the elastic interaction, G_{el}.

G_{mix} is given by the following expression [13, 14]:

$$\frac{G_{mix}}{kT} = \left(\frac{2{V_2}^2}{V_1}\right) {v_2}^2 \left(\frac{1}{2} - \chi\right) \left(\delta - \frac{h}{2}\right)^2 \left(3R + 2\delta + \frac{h}{2}\right) \tag{6}$$

where k is Boltzmann's constant, T is the absolute temperature, V_2 is the molar volume of polymer, V_1 is the molar volume of solvent, v_2 is the number of polymer chains per unit area, χ is the Flory–Huggins interaction parameter and δ is the hydrodynamic thickness of the adsorbed layer.

The sign of G_{mix} depends on the value of the Flory–Huggins interaction parameter χ: if $\chi < 0.5$, G_{mix} is positive and one obtains repulsion; if $\chi > 0.5$, G_{mix} is negative and one obtains attraction; if $\chi = 0.5$, $G_{mix} = 0$ and this is referred to as the θ-condition.

The elastic interaction is given by the following expression [15]:

$$\frac{G_{el}}{kT} = 2v_2 \ln\left[\frac{\Omega(h)}{\Omega(\infty)}\right] = 2v_2 R_{el}(h) \tag{7}$$

where $\Omega(h)$ is the number of configurations of the chains at separation distance h and $\Omega(\infty)$ is the value at $h = \infty$. $R_{el}(h)$ is a geometric function whose form

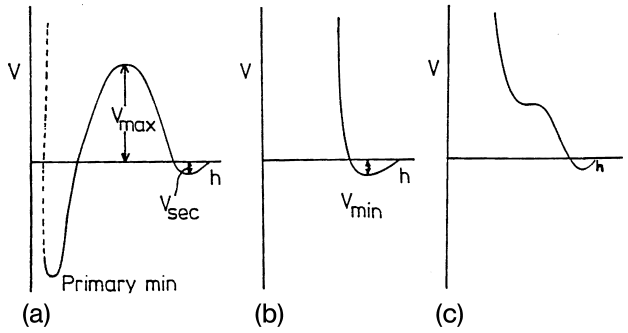

Figure 1.2 Energy–distance curves for electrostatic (a), steric (b) and electrosteric (c) systems.

depends on the chain segment distribution at the surface of the particle or droplet.

Combination of van der Waals attraction with double-layer repulsion forms the basis of the theory of colloid stability due to Deyaguin, Landau, Verwey and Overbeek (DLVO theory) [16, 17]. The force–distance curve according to the DLVO theory is represented schematically in Figure 1.2a. This shows two minima and one maximum. The minimum at long separation distances (secondary minimum, a few kT units) results in weak and reversible flocculation. This could be useful is some applications, e.g. reduction of formation of hard sediments or cream layers. The minimum at short distances (primary minimum, several hundred kT units) results in very strong (irreversible) flocculation. The maximum at intermediate distances (energy barrier) prevents aggregation into the primary minimum. To maintain kinetic stability of the dispersion (with long-term stability against strong flocculation) the energy barrier should be $>25kT$. The height of the energy barrier increases with decrease in electrolyte concentration, decrease in valency of the ions and increase of the surface or zeta potential.

Combination of van der Waals attraction with steric repulsion (combination of mixing and elastic interaction) forms the basis of the theory of steric stabilization [18]. Figure 1.2b gives a schematic representation of the force–distance curve of sterically stabilized systems. This force–distance curve shows a shallow minimum at a separation distance h comparable to twice the adsorbed layer thickness (2δ) and when $h < 2\delta$, very strong repulsion occurs. Unlike the V–h curve predicted by the DLVO theory (which shows two minima), the V–h curve of sterically stabilized systems shows only one minimum whose depth depends on the particle or droplet radius R, the Hamaker constant A and the adsorbed layer thickness δ. At given R and A, the depth of the minimum decreases with increase in the adsorbed layer thickness δ. When the latter exceeds a certain value (particularly with small particles or droplets) the minimum depth can become $<kT$ and the dispersion approaches thermodynamic stability. This forms the basis of the stability of nanodispersions.

Combination of the van der Waals attraction with double-layer and steric repulsion is illustrated schematically in Figure 1.2c and this is sometimes referred to

as electrosteric stabilization, as produced for example by the use of polyelectrolytes. This V–h curve has a minimum at long distances of separation, a shallow maximum at intermediate distances (due to double-layer repulsion) and a steep rise in repulsion at smaller h values (due to steric repulsion).

These energy–distance curves can be applied to describe some of the structures (states) produced in suspensions and emulsions. Figure 1.3 shows a schematic representation of the various states that may be produced in a suspension. One also has to consider the effect of gravity, which is very important when the particle size is relatively large (say >1 μm) and the density difference between the particles and the medium is significant (>0.1).

States (a) to (c) in Figure 1.3 represent the case for colloidally stable suspensions. In other words, the net interaction in the suspension is repulsive. Only state (a) with very small particles is physically stable. In this case the Brownian diffusion can overcome the gravity force and no sedimentation occurs; this is the

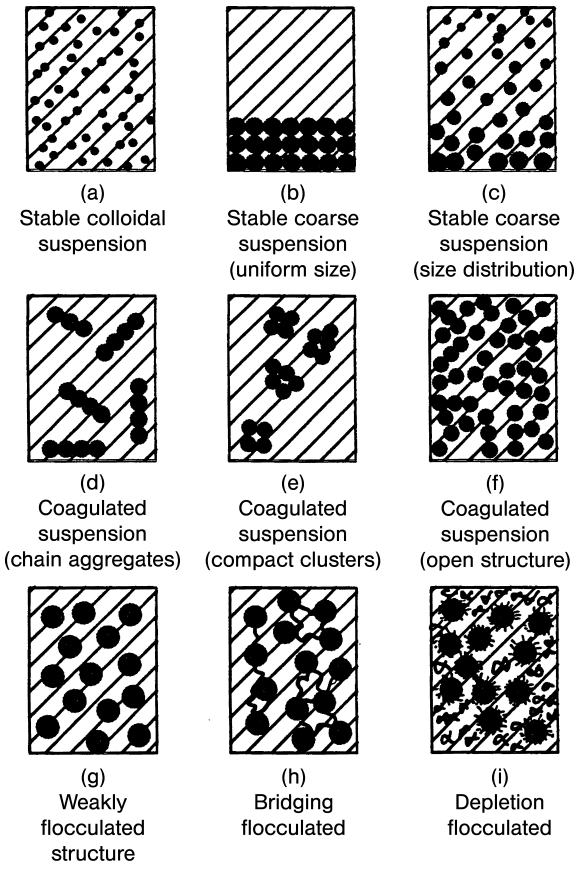

Figure 1.3 Different states of suspensions.

case with nanosuspensions (with size range 20–200 nm):

$$kT > \frac{4}{3}\pi R^3 \Delta\rho g L \tag{8}$$

where R is the particle radius, $\Delta\rho$ is the buoyancy (difference between particle density and that of the medium), g is the acceleration due to gravity and L is the height of the container.

States (b) and (c) are physically unstable (showing settling and formation of hard sediments), even though the system is colloidally stable. In this case the gravity force exceeds the Brownian diffusion:

$$kT \ll \frac{4}{3}\pi R^3 \Delta\rho g L \tag{9}$$

States (d) to (f) are strongly flocculated systems. In other words, the net interaction between the particles is attractive with a deep primary minimum. In state (d), chain aggregates are produced particularly under conditions of no stirring. These aggregates sediment under gravity, forming an ''open'' structure with the particles strongly held together. State (e) represents the case of formation of compact clusters which will also sediment forming a more ''compact'' structure again with the particles strongly held together. State (f) is the case of a highly concentrated suspension with the particles forming a strong three-dimensional ''gel'' structure that extends through the whole volume of the suspension. Such strongly flocculated structure (which is sometimes described as ''one-floc'') may undergo some contraction and some of the continuous phase may appear at the top, a phenomenon described as syneresis. Clearly, all these strongly flocculated structures must be avoided since the suspension cannot be redispersed on shaking.

The most important cases are those of (g) and (h), which represent reversible weakly flocculated systems. State (g) is the case of secondary minimum flocculation that prevents the formation of hard sediments. These weakly flocculated structures can be redispersed on shaking or on application and they sometimes show thixotropy (reduction of viscosity on application of shear and recovery of the viscosity when the shear is stopped). State (h) is produced by the addition of a weakly adsorbed high molecular weight polymer that causes bridging between the particles. Under conditions of incomplete coverage of the particles by the polymer chains, the latter become simultaneously adsorbed on two or more particles. If the adsorption of the polymeric chain is not strong, these polymer bridges can be broken under shear and the suspension may also show thixotropy. State (i) is a weakly flocculated suspension produced by the addition of ''free'' nonadsorbing polymer. Addition of a nonadsorbing polymer to a sterically stabilized suspension results in the formation of depletion zones (that are free of the polymer chains) around the particles. The free polymer chains cannot approach the surface of the particles since this will reduce entropy that is not compensated

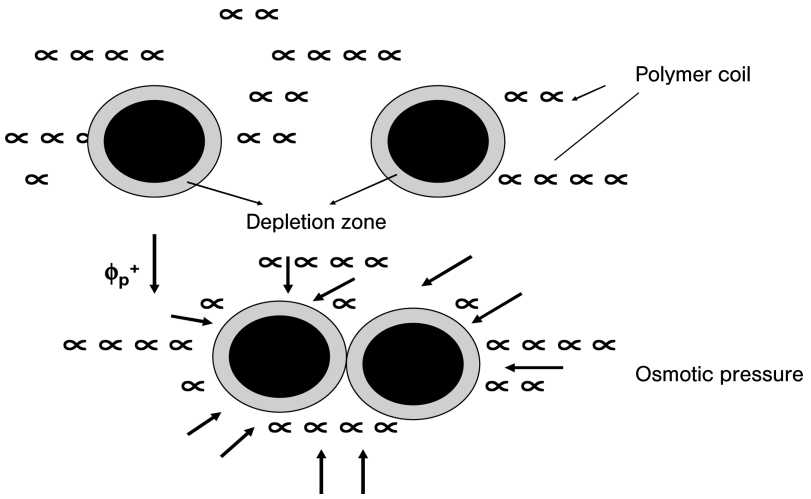

Figure 1.4 Schematic representation of depletion flocculation.

by an adsorption energy. On increasing the free polymer concentration or volume fraction ϕ_p above a critical value $\phi_p{}^+$, the depletion zones overlap and the polymer chains become "squeezed out" from between the particles. This results in an increase in the osmotic pressure outside the particles, resulting in a weak attraction that is referred to as depletion flocculation. A schematic representation of depletion flocculation is shown in Figure 1.4.

The magnitude of the depletion attraction energy G_{dep} is proportional to the polymer volume fraction ϕ_p and the molecular weight of the free polymer M. The range of depletion attraction is determined by the thickness Δ of the depletion zone, which is roughly equal to the radius of gyration of the free polymer, R_g.

G_{dep} is given by the following expression:

$$G_{dep} = \frac{2\pi R\Delta^2}{V_1}(\mu_1 - \mu_1{}^0)\left(1 + \frac{2\Delta}{R}\right) \tag{10}$$

where V_1 is the molar volume of the solvent, μ_1 the chemical potential of the solvent in the presence of free polymer with volume fraction ϕ_p and $\mu_1{}^0$ the chemical potential of the solvent in the absence of free polymer.

The different states of emulsions are illustrated schematically in Figure 1.5.

The states of emulsions represented in Figure 1.5 have some common features with suspensions. Creaming or sedimentation results from gravity, in which case the emulsion separates. If the emulsion droplet size is reduced to say 20–200 nm, the Brownian diffusion can overcome the gravity force and no separation occurs. This is the case with nanoemulsions. Emulsion flocculation can occur when there is not sufficient repulsion. Flocculation can be weak or strong depending on the magnitude of the attractive energy. Ostwald ripening of emulsions can

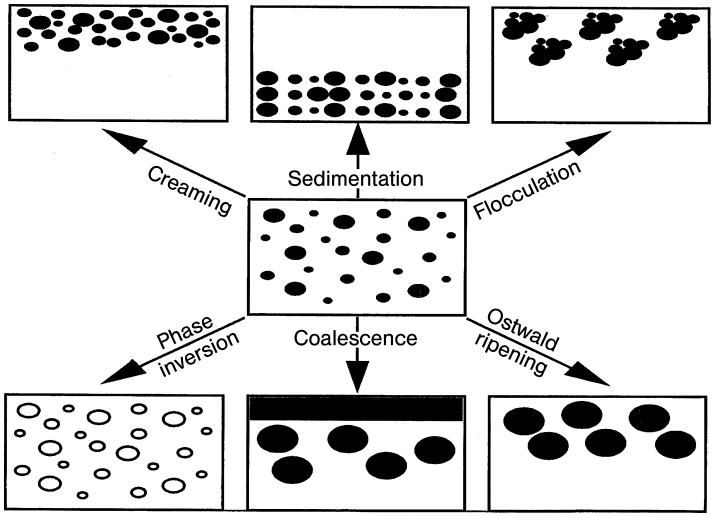

Figure 1.5 Different states of emulsions.

occur if the oil solubility is significant. The smaller droplets (with high radius of curvature) have higher solubility than larger droplets. This results in diffusion of the oil molecules from the small to the large droplets, resulting in an increase in the droplet size. Emulsion coalescence is the result of thinning and disruption of the liquid film between the droplets with the ultimate oil separation. Phase inversion can occur above a critical volume fraction of the disperse phase.

A number of the above instability problems with suspensions, emulsions and suspoemulsions can be overcome by using polymeric surfactants, which will be discussed later. For example, strong flocculation, coalescence and Ostwald ripening can be reduced or eliminated by the use of specially designed polymeric surfactants. Creaming or sedimentation can be eliminated by the use of ''thickeners'' that are sometimes referred to as ''rheology modifiers''.

1.3
Self-Assembly Structures in Cosmetic Formulations

Surfactant micelles and bilayers are the building blocks of most self-assembly structures. One can divide the phase structures into two main groups [19]: (1) those that are built of limited or discrete self-assemblies, which may be characterized roughly as spherical, prolate or cylindrical, and (2) infinite or unlimited self-assemblies whereby the aggregates are connected over macroscopic distances in one, two or three dimensions. The hexagonal phase (see below) is an example of one-dimensional continuity, the lamellar phase of two-dimensional continuity, whereas the bicontinuous cubic phase and the sponge phase (see later) are exam-

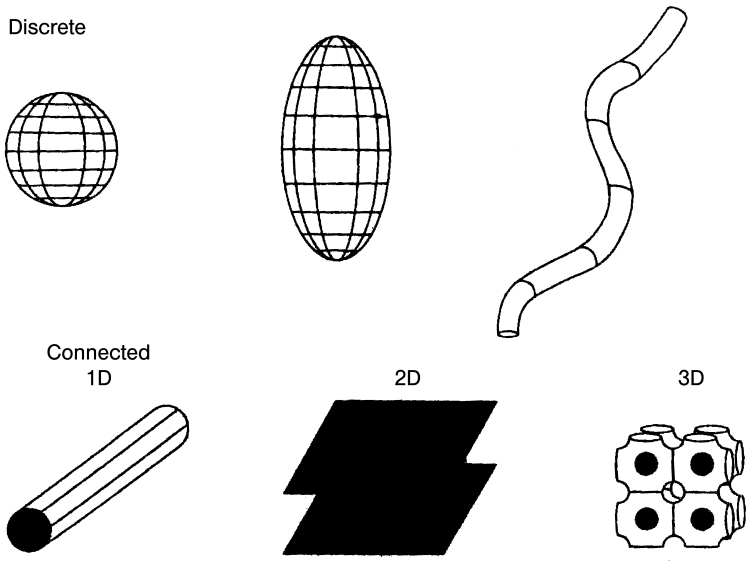

Figure 1.6 Schematic representation of self-assembly structures.

ples of three-dimensional continuity. These two types are illustrated schematically in Figure 1.6.

1.4
Structure of Liquid Crystalline Phases

The above-mentioned unlimited self-assembly structures in 1D, 2D or 3D are referred to as liquid crystalline structures. The last type behave as fluids and are usually highly viscous. At the same time, X-ray studies of these phases yield a small number of relatively sharp lines which resemble those produced by crystals [20]. Since they are fluids they are less ordered than crystals, but because of the X-ray lines and their high viscosity it is also apparent that they are more ordered than ordinary liquids. Thus, the term liquid crystalline phase is very appropriate for describing these self-assembled structures. Below, a brief description of the various liquid crystalline structures that can be produced with surfactants is given and Table 1.1 shows the most commonly used notation to describe these systems.

1.4.1
Hexagonal Phase

This phase is built up of (infinitely) long cylindrical micelles arranged in a hexagonal pattern, with each micelle being surrounded by six other micelles, as

Table 1.1 Notation of the most common liquid crystalline structures.

Phase structure	Abbreviation	Notation
Micellar	mic	L_1, S
Reversed micellar	rev mic	L_2, S
Hexagonal	hex	H_1, E, M_1, middle
Reversed hexagonal	rev hex	H_2, F, M_2
Cubic (normal micellar)	cub_m	I_1, S_{1c}
Cubic (reversed micelle)	cub_m	I_2
Cubic (normal bicontinuous)	cub_b	I_1, V_1
Cubic (reversed bicontinuous)	cub_b	I_2, V_2
Lamellar	lam	L_α, D, G, neat
Gel	gel	L_β
Sponge phase (reversed)	spo	L_3 (normal), L_4

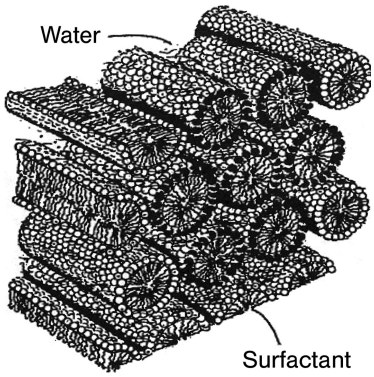

Figure 1.7 Schematic representation of the hexagonal phase.

shown schematically in Figure 1.7. The radius of the circular cross-section (which may be somewhat deformed) is again close to the surfactant molecule length [21].

1.4.2 Micellar Cubic Phase

This phase is built up of a regular packing of small micelles, which have similar properties to small micelles in the solution phase. However, the micelles are short prolates (axial ratio 1–2) rather than spheres, since this allows better packing. The micellar cubic phase is highly viscous. A schematic representation of the micellar cubic phase [22] is shown in Figure 1.8.

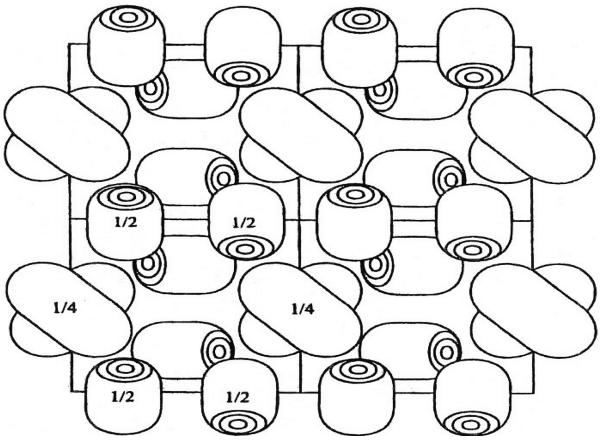

Figure 1.8 Representation of the micellar cubic phase.

1.4.3 Lamellar Phase

This phase is built of bilayers of surfactant molecules alternating with water layers. The thickness of the bilayers is somewhat smaller than twice the surfactant molecule length. The thickness of the water layer can vary over wide ranges, depending on the nature of the surfactant. The surfactant bilayer can range from being stiff and planar to being very flexible and undulating. A schematic representation of the lamellar phase [21] is shown in Figure 1.9.

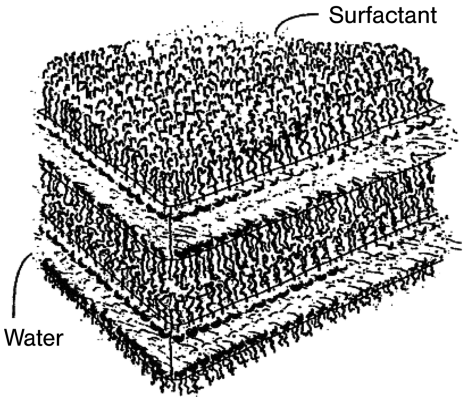

Figure 1.9 Schematic representation of the lamellar phase [7].

1.4.4
Discontinuous Cubic Phases

These phases can be a number of different structures, where the surfactant molecules form aggregates that penetrate space, forming a porous connected structure in three dimensions. They can be considered as structures formed by connecting rod-like micelles (branched micelles) or bilayer structures [23].

1.4.5
Reversed Structures

Except for the lamellar phase, which is symmetrical around the middle of the bilayer, the different structures have a reversed counterpart in which the polar and non-polar parts have changed roles. For example, a hexagonal phase is built up of hexagonally packed water cylinders surrounded by the polar head groups of the surfactant molecules and a continuum of the hydrophobic parts. Similarly, reversed (micellar-type) cubic phases and reversed micelles consist of globular water cores surrounded by surfactant molecules. The radii of the water cores are typically in the range 2–10 nm.

1.5
Driving Force for Formation of Liquid Crystalline Phases

One of the simplest methods for predicting the shape of an aggregated structure is based on the critical packing parameter P [8].

For a spherical micelle with radius r and containing n molecules each with volume v and cross-sectional area a_0:

$$n = \frac{4\pi r^3}{3v} = \frac{4\pi r^2}{a_0} \tag{11}$$

$$a_0 = \frac{3v}{r} \tag{12}$$

The cross-sectional area of the hydrocarbon tail, a, is given by

$$a = \frac{v}{l_c} \tag{13}$$

where l_c is the extended length of the hydrocarbon tail.

$$P = \frac{a}{a_0} = \frac{1}{3}\frac{r}{l_c} \tag{14}$$

Since $r < l_c$, then $P < 1/3$.

For a cylindrical micelle with radius r and length d:

$$n = \frac{\pi r^r d}{v} = \frac{2\pi r d}{a_0} \tag{15}$$

$$a_0 = \frac{2v}{r} \tag{16}$$

$$P = \frac{a}{a_0} = \frac{1}{2}\frac{r}{l_c} \tag{17}$$

Since $r < l_c$, $1/3 < P < 1/2$. For liposomes and vesicles $1 > P > 2/3$; for lamellar micelles $P \approx 1$; and for reverse micelles $P > 1$.

The packing parameter can be controlled by using mixtures of surfactants to arrive at the most desirable structure.

The most useful liquid crystalline structures in personal care applications are those of the lamellar phase. These lamellar phases can be produced in emulsion systems by using a combination of surfactants with various HLB numbers and choosing the right oil (emollient). In many cases, liposomes and vesicles are also produced by using lipids of various compositions. Two main types of lamellar liquid crystalline structures can be produced: "oleosomes" and "hydrosomes" (Figure 1.10).

Several advantages of lamellar liquid crystalline phases in cosmetics can be quoted: (1) they produce an effective barrier against coalescence; (2) they can produce "gel networks" that provide the right consistency for application in addition to preventing creaming or sedimentation; (3) they can influence the delivery of active ingredients of both the lipophilic and hydrophilic types; (4) since they mimic the skin structure (in particular the stratum corneum), they can offer prolonged hydration potential.

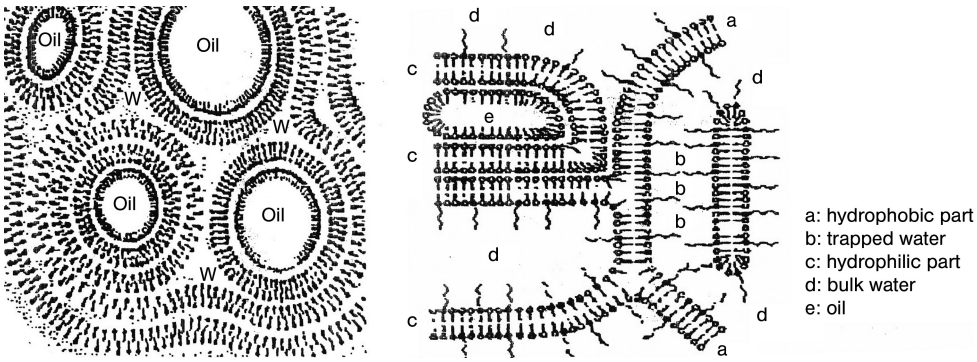

Figure 1.10 Schematic representation of "oleosomes" and "hydrosomes".

1.6
Polymeric Surfactants in Cosmetic Formulations

Polymeric surfactants of the A–B, A–B–A block or BA_n (or AB_n) graft types (where B is the "anchor" chain and A is the "stabilizing" chain) offer more robust stabilizing systems for dispersions (suspensions and emulsions) in cosmetics: (1) the high molecular weight of the surfactant (>1000) ensures strong adsorption of the molecule (no desorption); (2) the strong hydration of the A chain(s) ensures effective steric stabilization; (3) a lower emulsifier or dispersant concentration is sufficient (usually one order of magnitude lower than low molecular weight surfactants); (4) this lower concentration and high molecular weight of the material ensure the absence of any skin irritation.

One of the earliest polymeric surfactants used is the A–B–A block copolymer of poly(ethylene oxide) (PEO, A) and propylene oxide (PPO, B): Pluronics, Synperonic PE or Poloxamers. These are not ideal since adsorption by the PPO chain is not strong.

Recently, ORAFTI (Belgium) developed a polymeric surfactant based on inulin (a natural, linear polyfructose molecule produced from chicory roots) [24]. By grafting several alkyl chains on the polyfructose chain, a graft copolymer was produced (Figure 1.11).

The alkyl chains are strongly adsorbed at the oil or particle surface, leaving loops of polyfructose in the aqueous continuous phase (Figure 1.12). The polyfructose loops extend in solution (giving a layer thickness in the region of 10 nm) and they are highly solvated by the water molecules (solvation forces). The loops remain hydrated at high temperatures (>50 °C) and also in the presence of high electrolyte concentrations (up to 4 mol dm^{-3} NaCl and 1.5 mol dm^{-3} $MgSO_4$. Several O/W emulsions were prepared using INUTEC SP1 at a concentration of 1% for a 50:50 v/v emulsion. Hydrocarbon and silicone oils were used and the emulsions were prepared in water, 2 mol dm^{-3} NaCl and 1 mol dm^{-3} $MgSO_4$. All emulsions were stable against coalescence at room temperature and 50 °C for more than 1 year. The high stability of the emulsions is due to the unfavorable mixing of the strongly hydrated polyfructose loops (osmotic repulsion).

The multipoint anchoring of the polymer chains also ensures strong elastic (entropic) repulsion. This provides enhanced steric stabilization.

Evidence for the high stability of emulsions when using INUTEC SP1 has recently been obtained [25] from disjoining pressure measurements between two

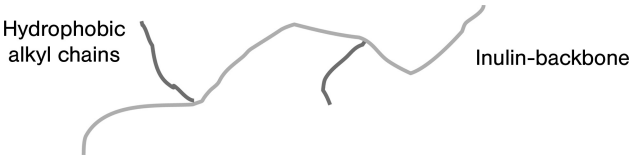

Figure 1.11 Hydrophobically modified inulin (HMI): INUTEC SP1.

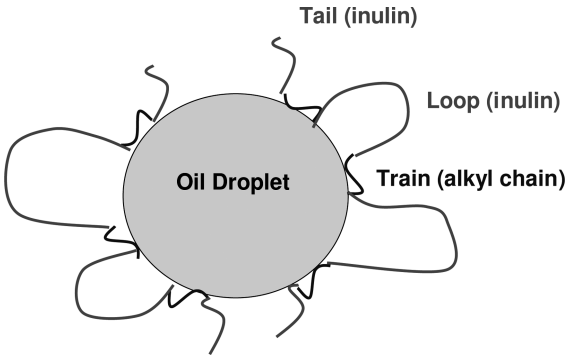

Figure 1.12 Schematic representation of the adsorption and conformation of INUTEC SP1 on oil droplets in aqueous medium.

oil droplets containing adsorbed polymer surfactant both in water and in high electrolyte solutions. A schematic representation of the measuring cell developed by Exerowa and Kruglyakov [26] is shown in Figure 1.13. A porous plate is used to produce a thin film with radius r between two oil droplets and the capillary pressure can be gradually increased to values reaching 45 kPa.

Figure 1.14 shows the variation of disjoining pressure with film thickness at various NaCl concentrations. It can be seen that by increasing the capillary pressure a stable Newton black film (NBF) is obtained at a film thickness of ~7 nm. The lack of rupture of the NBF up to the highest pressure applied, namely 4.5×10^4 Pa, clearly indicates the high stability of the liquid film in the presence of high NaCl concentrations (2 mol dm^{-3}). This result is consistent with the high emulsion stability obtained at high electrolyte concentrations and high temperature. Emulsions of Isopar M in water are very stable under such conditions and this could be accounted for by the high stability of the NBF. The droplet size of 50:50 O/W emulsions prepared using 2% INUTEC SP1 is in the range 1–10 μm. This corresponds to a capillary pressure of $\sim 3 \times 10^4$ Pa for 1-μm drops and $\sim 3 \times 10^3$ Pa for 10-μm drops. These capillary pressures are lower than those to which the NBF has been subjected and this clearly indicates the high stability obtained against coalescence in these emulsions.

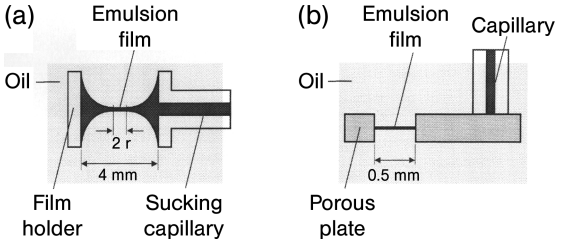

Figure 1.13 Schematic representation of Emulsion film stability measurement.

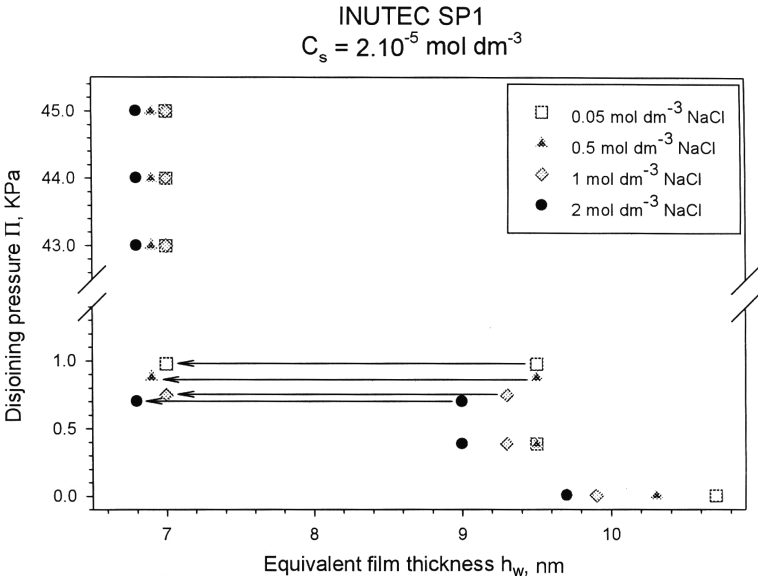

Figure 1.14 Variation of disjoining pressure with film thickness at various NaCl concentrations.

The graft copolymer INUTEC SP1 can also be used for the stabilization of hydrophobic particles in aqueous media. The alkyl chains are strongly adsorbed on the particle surface with multi-point attachment leaving the strongly hydrated polyfructose loops and tails dangling in solution, thus providing an effective steric barrier. Evidence for this high stability obtained using INUTEC SP1 has been obtained using atomic force microscopy (AFM) measurements [27] between a hydrophobically modified glass sphere and a plate both containing an adsorbed layer of INUTEC SP1. Results were obtained both in water and in various Na_2SO_4 solutions. Figure 1.15 shows the variation of force with separation distance

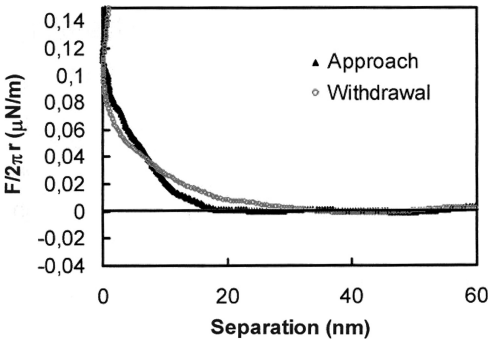

Figure 1.15 Force–distance curves between hydrophobized glass surfaces containing adsorbed INUTEC SP1 in water.

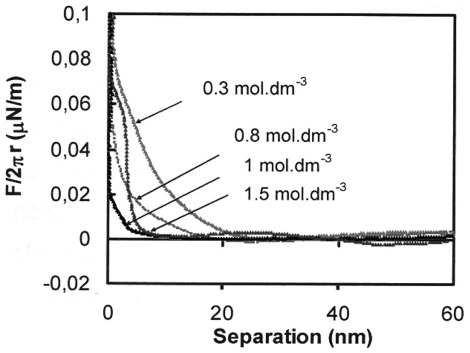

Figure 1.16 Force–distance curves for hydrophobized glass surfaces containing adsorbed INUTEC SP1 at various Na_2SO_4 concentrations.

between the glass sphere and plate in aqueous solutions containing INUTEC SP1 at the saturation adsorption concentration. The results at various Na_2SO_4 concentrations are shown in Figure 1.16.

It can be seen from Figure 1.15 that the force between the hydrophobized glass surface containing adsorbed INUTEC SP1 starts to increase at a separation distance of ~20 nm, which corresponds to an adsorbed layer thickness of ~10 nm. The above thickness is maintained in 0.3 mol dm^{-3} Na_2SO_4 (Figure 1.16). With increasing Na_2SO_4 concentration the adsorbed layer thickness decreases, reaching ~3 nm in the presence of 1.5 mol dm^{-3} Na_2SO_4. Even at such a high electrolyte concentration, the interaction is still repulsive.

1.7
Polymeric Surfactants for Stabilization of Nanoemulsions

Nanoemulsions are transparent or translucent systems in the size range 20–200 nm [28]. Whether the system is transparent or translucent depends on the droplet size, the volume fraction of the oil and the refractive index difference between the droplets and the medium. Nanoemulsions having diameters < 50 nm appear transparent when the oil volume fraction is <0.2 and the refractive index difference between the droplets and the medium is not large. With increase in droplet diameter and oil volume fraction the system may appear translucent and at higher oil volume fractions the system may become turbid.

Nanoemulsions are only kinetically stable. They have to be distinguished from microemulsions (that cover the size range 5–50 nm), which are mostly transparent and thermodynamically stable. The long-term physical stability of nanoemulsions (with no apparent flocculation or coalescence) makes them unique and they are sometimes referred to as ''approaching thermodynamic stability''. The inherently high colloid stability of nanoemulsions can be well understood from consideration of their steric stabilization (when using nonionic surfactants and/

or polymers) and how this is affected by the ratio of the adsorbed layer thickness to droplet radius, as will be discussed below.

Unless adequately prepared (to control the droplet size distribution) and stabilized against Ostwald ripening (that occurs when the oil has some finite solubility in the continuous medium), nanoemulsions may show an increase in the droplet size and an initially transparent system may become turbid on storage.

The attraction of nanoemulsions for application in personal care and cosmetics is due to the following advantages: (1) the very small droplet size causes a large reduction in the gravity force and the Brownian motion may be sufficient for overcoming gravity; this means that no creaming or sedimentation occurs on storage; (2) the small droplet size also prevents any flocculation of the droplets; weak flocculation is prevented and this enables the system to remain dispersed with no separation; (3) the small droplets also prevent their coalescence, since these droplets are non-deformable and hence surface fluctuations are prevented; in addition, the significant surfactant film thickness (relative to droplet radius) prevents any thinning or disruption of the liquid film between the droplets; (4) nanoemulsions are suitable for efficient delivery of active ingredients through the skin – the large surface area of the emulsion system allows rapid penetration of actives; (5) due to their small size, nanoemulsions can penetrate through the "rough" skin surface and this enhances penetration of actives; (6) the transparent nature of the system, their fluidity (at reasonable oil concentrations) and the absence of any thickeners may give them a pleasant esthetic character and skin feel; (7) unlike microemulsions (which require a high surfactant concentration, usually in the region of 20% and higher), nanoemulsions can be prepared using reasonable surfactant concentrations; for a 20% O/W nanoemulsion, a surfactant concentration in the range 5–10% may be sufficient; (8) the small size of the droplets allows them to deposit uniformly on substrates; wetting, spreading and penetration may be also enhanced as a result of the low surface tension of the whole system and the low interfacial tension of the O/W droplets; (9) nanoemulsions can be applied for delivery of fragrants which may be incorporated in many personal care products; this could also be applied in perfumes which are desirable to be formulated alcohol free; (10) nanoemulsions may be applied as a substitute for liposomes and vesicles (which are much less stable) and it is possible in some cases to build lamellar liquid crystalline phases around the nanoemulsion droplets.

The inherently high colloid stability of nanoemulsions when using polymeric surfactants is due to their steric stabilization. The mechanism of steric stabilization was discussed before. As shown in Figure 1.2a, the energy distance curve shows a shallow attractive minimum at a separation distance comparable to twice the adsorbed layer thickness 2δ. This minimum decreases in magnitude as the ratio of adsorbed layer thickness to droplet size increases. With nanoemulsions the ratio of adsorbed layer thickness to droplet radius (δ/R) is relatively large (0.1–0.2) compared with macroemulsions. This is illustrated schematically in Figure 1.17, which shows the reduction in G_{min} with increase in δ/R.

These systems approach thermodynamic stability against flocculation and/or coalescence. The very small size of the droplets and the dense adsorbed layers

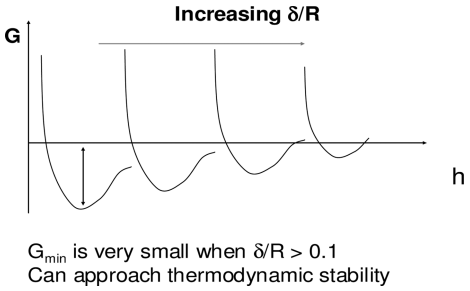

Figure 1.17 Importance of the ratio of adsorbed layer thickness to particle size.

ensure lack of deformation of the interface and lack of thinning, and disruption of the liquid film between the droplets and hence coalescence is also prevented.

One of the main problems with nanoemulsions is Ostwald ripening, which results from the difference in solubility between small and large droplets [28]. The difference in chemical potential of dispersed phase droplets between different sized droplets was given by Lord Kelvin:

$$c(r) = c(\infty)\exp\left(\frac{2\gamma V_m}{rRT}\right) \tag{18}$$

where $c(r)$ is the solubility surrounding a particle of radius r, $c(\infty)$ is the bulk phase solubility and V_m is the molar volume of the dispersed phase. The quantity $2\gamma V_m/RT$ is termed the characteristic length. It has an order of $\sim$1 nm or less, indicating that the difference in solubility of a 1-μm droplet is of the order of 0.1% or less.

Theoretically, Ostwald ripening should lead to condensation of all droplets into a single drop (i.e. phase separation). This does not occur in practice since the rate of growth decreases with increase in droplet size.

For two droplets of radii r_1 and r_2 (where $r_1 < r_2$):

$$\frac{RT}{V_m}\ln\left[\frac{c(r_1)}{c(r_2)}\right] = 2\gamma\left(\frac{1}{r_1} - \frac{1}{r_2}\right) \tag{19}$$

Equation (19) shows that the larger the difference between r_1 and r_2, the higher is the rate of Ostwald ripening.

Ostwald ripening can be quantitatively assessed from plots of the cube of the radius versus time t [28]:

$$r^3 = \frac{8}{9}\left[\frac{c(\infty)\gamma V_m}{\rho RT}\right]t \tag{20}$$

where D is the diffusion coefficient of the disperse phase in the continuous phase.

Ostwald ripening can be reduced by incorporation of a second component which is insoluble in the continuous phase (e.g. squalane). In this case, significant partitioning between different droplets occurs, with the component having low solubility in the continuous phase expected to be concentrated in the smaller droplets. During Ostwald ripening in a two-component disperse phase system, equilibrium is established when the difference in chemical potential between different sized droplets (which results from curvature effects) is balanced by the difference in chemical potential resulting from partitioning of the two components. If the secondary component has zero solubility in the continuous phase, the size distribution will not deviate from the initial one (the growth rate is equal to zero). In the case of limited solubility of the secondary component, the distribution is the same as governed by Eq. (19), i.e. a mixture growth rate is obtained which is still lower than that of the more soluble component.

The above method is of limited application since one requires a highly insoluble oil as the second phase which is miscible with the primary phase.

Another method for reducing Ostwald ripening depends on modification of the interfacial film at the O/W interface. According to Eq. (19), a decrease in γ results in a reduction of Ostwald ripening. However, this alone is not sufficient since one has to reduce γ by several orders of magnitude. It has been suggested that by using surfactants which are strongly adsorbed at the O/W interface (i.e. polymeric surfactants) and which do not desorb during ripening, the rate could besignificantly reduced. An increase in the surface dilatational modulus and decrease in γ would be observed for the shrinking drops. The difference in γ between the droplets would balance the difference in capillary pressure (i.e. curvature effects).

To achieve the above effect, it is useful to use A–B–A block copolymers that are soluble in the oil phase and insoluble in the continuous phase. A strongly adsorbed polymeric surfactant that has limited solubility in the aqueous phase can also be used [e.g. hydrophobically modified inulin, INUTEC SP1 (ORAFTI, Belgium], as will be discussed below.

Two methods may be applied for the preparation of nanoemulsions (covering the droplet radius size range 20–200 nm): use of high-pressure homogenizers (aided by appropriate choice of surfactants and cosurfactants) or application of the phase inversion temperature (PIT) concept. The production of small droplets (submicron) requires the application of high energy. The process of emulsification is generally inefficient, as illustrated below. Simple calculations show that the mechanical energy required for emulsification exceeds the interfacial energy by several orders of magnitude. For example, to produce a nanoemulsion at $\varphi = 0.1$ with an average radius R of 200 nm, using a surfactant that gives an interfacial tension $\gamma = 10\ \text{mN m}^{-1}$, the net increase in surface free energy is $A\gamma = 3\varphi\gamma/R = 1.5 \times 10^4\ \text{J m}^{-3}$. The mechanical energy required in a homogenizer is $1.5 \times 10^7\ \text{J m}^{-3}$, i.e. an efficiency of 0.1%. The rest of the energy (99.9%) is dissipated as heat.

The intensity of the process or the effectiveness in making small droplets is often governed by the net power density $[\varepsilon(t)]$:

$$p = \varepsilon(t)\,\mathrm{d}t \tag{21}$$

where t is the time during which emulsification occurs.

Break-up of droplets will only occur at high ε values, which means that the energy dissipated at low ε levels is wasted. Batch processes are generally less efficient than continuous processes. This shows why with a stirrer in a large vessel, most of the energy applies at low intensity is dissipated as heat. In a homogenizer, p is simply equal to the homogenizer pressure.

Several procedures may be applied to enhance the efficiency of emulsification when producing nanoemulsions: (1) one should optimize the efficiency of agitation by increasing ε and decreasing the dissipation time; (2) the nanoemulsion is preferably prepared at high volume faction of the disperse phase and subsequently diluted; however, very high φ values may result in coalescence during emulsification; (3) add more surfactant, whereby creating a smaller γ_{eff} and possibly diminishing recoalescence; (4) use a surfactant mixture that shows a greater reduction in γ than the individual components; (5) if possible dissolve the surfactant in the oil phase, which produces smaller droplets; (6) it may be useful to emulsify in steps of increasing intensity, particularly with nanoemulsions having highly viscous disperse phase.

Low-energy techniques may be applied for the preparation of nanoemulsions. Two methods can be applied: (1) the emulsifier is dissolved in the oil phase and the aqueous phase is gradually added; initially a W/O emulsion is produced but at a critical volume fraction of the aqueous phase inversion occurs and the resulting O/W system may form sufficiently small droplets in the nano-size range; (2) the phase inversion temperature (PIT) technique, which is by far the most suitable method for producing a nanoemulsion; it is limited to systems that contain an ethoxylated surfactant.

When an O/W emulsion prepared using a nonionic surfactant of the ethoxylate type is heated, then at a critical temperature (the PIT), the emulsion inverts to a W/O emulsion. At the PIT the hydrophilic and lipophilic components of the surfactant are exactly balanced and the PIT is sometimes referred to as the HLB temperature. At the PIT the droplet size reaches a minimum and the interfacial tension also reaches a minimum. However, the small droplets are unstable and they coalesce very rapidly.

By rapid cooling of the emulsion that is prepared at a temperature near the PIT, very stable nanoemulsion droplets could be produced. Near the HLB temperature, the interfacial tension reaches a minimum.

Several experiments were carried to investigate the methods of preparation of nanoemulsions and their stability. The first method applied the PIT principle for the preparation of nanoemulsions. Experiments were carried out using hexadecane as the oil phase and Brij 30 ($C_{12}EO_4$) as the nonionic emulsifier. The HLB temperature was determined using conductivity measurements, whereby 10^{-2} mol dm^{-3} NaCl was added to the aqueous phase (to increase the sensitivity of the conductibility measurements).

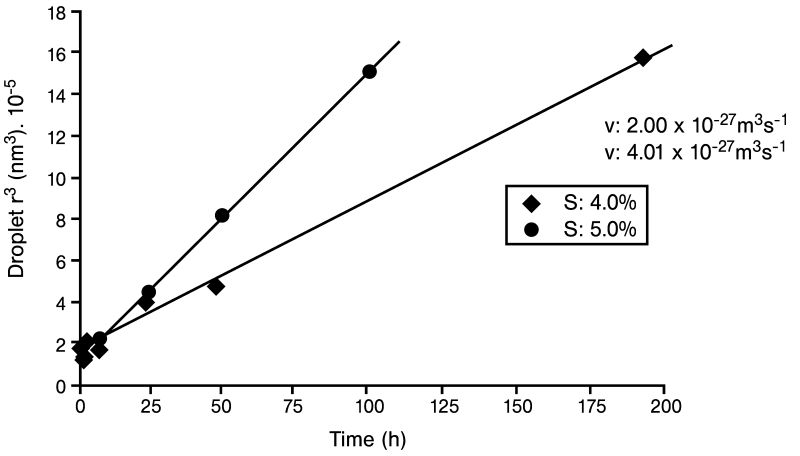

Figure 1.18 Variation of r^3 with time for hexadecane–water emulsions prepared using the PIT method.

Nanoemulsions were prepared by rapid cooling of the system to 25 °C. The droplet diameter was determined using photon correlation spectroscopy (PCS). At 4 and 5% surfactant, the average droplet diameter was 116 and 95 nm, respectively. However, the nanoemulsions showed significant polydispersity (polydispersity index of 0.29 and 0.09 at 4 and 5% surfactant, respectively). Nanoemulsions could not be produced when the surfactant concentration was reduced to below 4%. Nanoemulsions were then prepared using a high-pressure homogenizer (Emulsiflex) and these were smaller in size and much less polydisperse. For example, using 4% surfactant and 20% O/W emulsion, the average droplet diameter was 69 nm with a very low polydispersity index.

Figure 1.18 shows the variation of r^3 with time t for 20:80 O/W nanoemulsions at two $C_{12}EO_4$ concentrations prepared by the PIT method. It can be seen that the emulsion containing the higher surfactant concentration gives a higher rate of Ostwald ripening. This may be due to solubilization of the oil by the surfactant micelles.

Since the driving force for Ostwald ripening is the difference in solubility between smaller and larger droplets, one would expect that the narrower the droplet size distribution, the slower the rate. This is illustrated in Figure 1.19, which shows the variation of r^3 with time for nanoemulsions prepared using the PIT method and the homogenizer. It can be seen that the rate of Ostwald ripening is smaller for nanoemulsions prepared using the homogenizer when compared with the rate obtained using the PIT method.

Further evidence for Ostwald ripening was obtained by using a more soluble oil, namely a branched hexadecane (Arlamol HD). The results are shown in Figure 1.20 for nanoemulsions prepared using 4% surfactant. It can be seen that

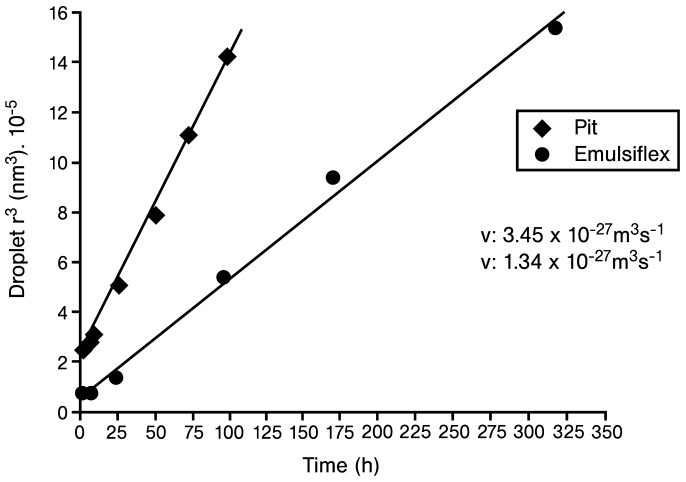

Figure 1.19 Comparison of Ostwald ripening using the PIT method and the Emulsiflex.

the more soluble oil (Arlamol HD) give a higher rate of Ostwald ripening when compared with a less soluble oil such as hexadecane.

As mentioned above, polymeric surfactants can reduce Ostwald ripening by enhancing the Gibbs elasticity at the O/W interface. Hydrophobically modified inulin (INUTEC SP1) is ideal for reduction of Ostwald ripening due to its strong adsorption and its limited solubility in the aqueous phase (no desorption occurs). This is illustrated in Figure 1.21, which shows plots of R^3 versus time for 20% v/v silicone O/W emulsions at two concentrations of INUTEC SP1. The concen-

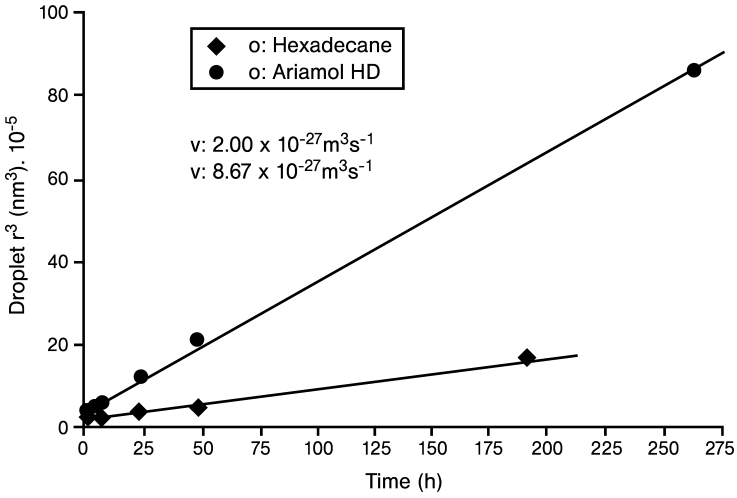

Figure 1.20 Ostwald ripening for hexadecane and Arlamol HD nanoemulsions.

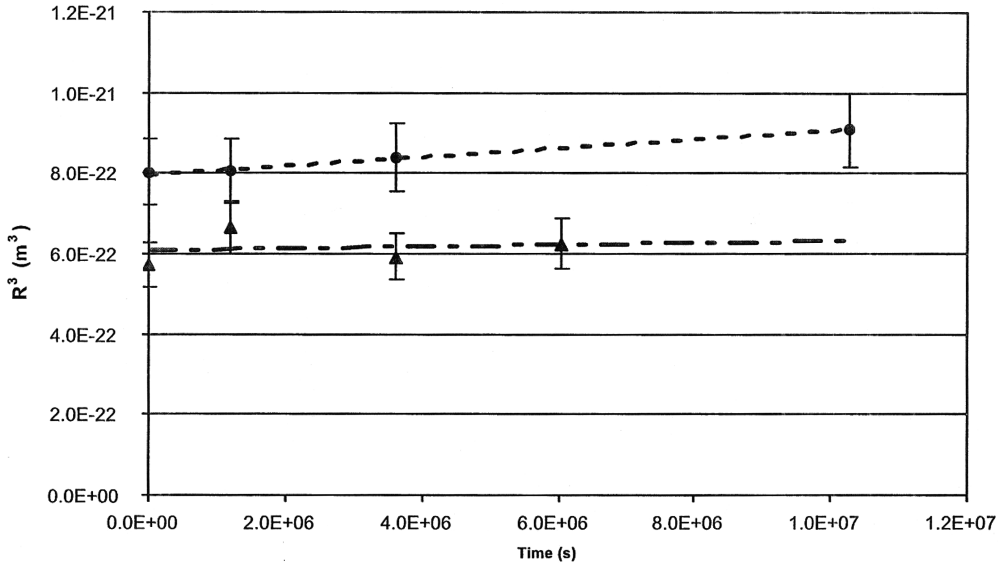

Figure 1.21 R^3 versus time for nanoemulsions at 1.6 and 2.4% HMI.

tration of INUTEC SP1 is much lower than that required when using nonionic surfactants.

The rate of Ostwald ripening is 1.1×10^{-29} and 2.4×10^{-30} $m^3\ s^{-1}$ at 1.6 and 2.4% INUTEC SP1, respectively. These rates are about three orders of magnitude lower than those obtained using a nonionic surfactant. Addition of 5% glycerol was found to decrease the rate of Ostwald ripening in some nanoemulsions.

The above systems of nanoemulsions are attractive for cosmetic applications: (1) low viscosity for application in sprayables; (2) efficient delivery of active ingredients through the skin; (3) ability to penetrate through the "rough" skin surface.

Various nanoemulsions with hydrocarbon oils of different solubility were prepared using INUTEC SP1. Figure 1.22 shows plots of r^3 versus t for nanoemulsions of the hydrocarbon oils that were stored at 50 °C. It can be seen that both paraffinum liquidum with low and high viscosity give almost a zero slope, indicating the absence of Ostwald ripening in this case. This is not surprising since both oils have very low solubility and the hydrophobically modified inulin, INUTEC SP1, strongly adsorbs at the interface, giving high elasticity that reduces both Ostwald ripening and coalescence.

With the more soluble hydrocarbon oils, namely isohexadecane, there is an increase in r^3 with time, giving a rate of Ostwald ripening of 4.1×10^{-27} $m^3\ s^{-1}$. The rate for this oil is almost three orders of a magnitude lower than that obtained with a nonionic surfactant, namely laureth-4 (C_{12}-alkyl chain with 4 mol of ethylene oxide) when the nanoemulsion was stored at 50 °C. This clearly shows the effectiveness of INUTEC SP1 in reducing Ostwald ripening. This reduction can be attributed to the enhancement of the Gibbs dilatational

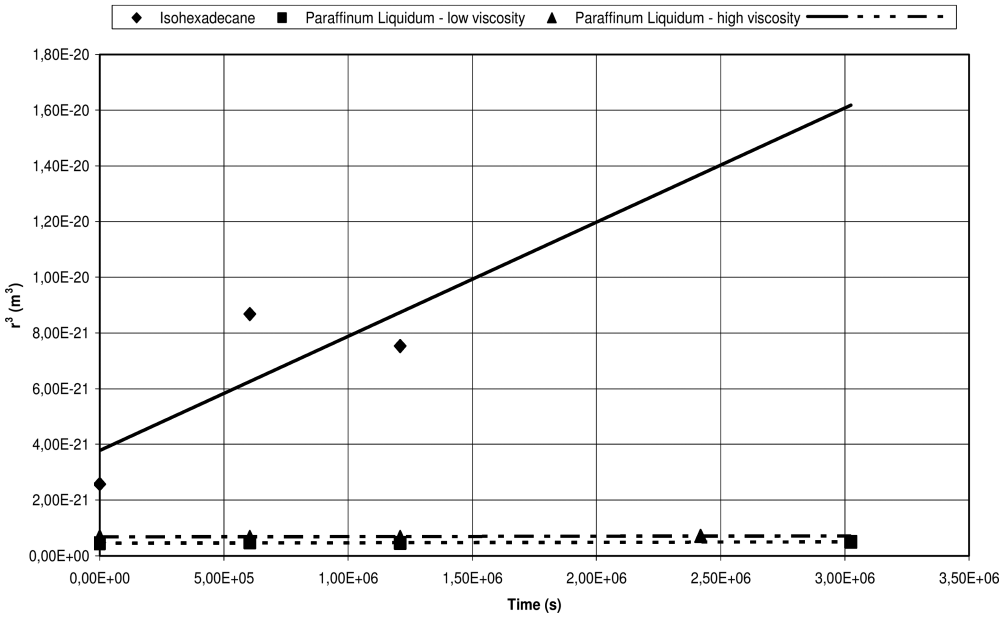

Figure 1.22 r^3 versus t for nanoemulsions based on hydrocarbon oils.

elasticity which results from the multi-point attachment of the polymeric surfactant with several alkyl groups to the oil droplets. This results in a decrease in the molecular diffusion of the oil from the smaller to the larger droplets.

1.8 Polymeric Surfactants in Multiple Emulsions

Multiple emulsions are complex systems of emulsions of emulsions [29, 30]: water-in-oil-in-water (W/O/W) and oil-in-water-in-oil (O/W/O). The W/O/W multiple emulsions are the most commonly used systems in personal care products. Multiple emulsions are ideal systems for application in cosmetics: (1) one can dissolve actives in three different compartments; (2) they can be used for controlled and sustained release; (3) they can be applied as creams by using thickeners in the outer continuous phase.

Multiple emulsions are conveniently prepared by a two-step process. For W/O/W, a W/O emulsion is first prepared using a low-HLB polymeric surfactant using a high-speed stirrer to produce droplets of ~1 μm. The W/O emulsion is then emulsified in an aqueous solution containing a high-HLB polymeric surfactant using a low-speed stirrer to produce droplets of 10–100 μm.

To prepare a stable multiple emulsion, the following criteria must be satisfied: (1) two emulsifiers with low and high HLB numbers to produce the primary W/O

emulsion and the final W/O/W multiple emulsion; (2) polymeric emulsifiers that provide steric stabilization are necessary to maintain the long-term physical stability; (3) optimum osmotic balance for W/O/W between the internal water droplets and outer continuous phase, which can be achieved by using electrolytes or non-electrolytes.

Multiple emulsions are conveniently prepared using a two step process: a W/O system is first prepared by emulsification of the aqueous phase (which may contain an electrolyte to control the osmotic pressure) into an oil solution of the polymeric surfactant with the low HLB number – a high-speed stirrer is used to produce droplets of ~1 μm. The droplet size of the primary emulsion can be determined using dynamic light scattering. The primary W/O emulsion is then emulsified into an aqueous solution (of an electrolyte to control the osmotic pressure) containing the polymeric surfactant with high HLB number – in this case a low-speed stirrer is used to produce multiple emulsion droplets in the range 10–100 μm. The droplet size of the multiple emulsion can be determined using optical microscopy (with image analysis) or using light diffraction techniques (Malvern Mastersizer). A schematic representation of the preparation of W/O/W multiple emulsions is shown in Figure 1.23.

A W/O/W multiple emulsion was prepared using two polymeric surfactants. A W/O emulsion was prepared using an A–B–A block copolymer of poly(hydroxystearic acid) (PHS, A) and poly(ethylene oxide) (PEO, B), i.e. PHS–PEO–PHS (Arlacel P135, UNIQEMA). This emulsion was prepared using a high-speed mixer giving droplet sizes in the region of 1 μm. The W/O emulsion was then emulsified in an aqueous solution of INUTEC SP1 using low-speed stirring to produce multiple emulsion droplets in the range 10–100 μm. The osmotic balance was achieved using 0.1 mol dm^{-3} $MgCl_2$ in the internal water droplets and

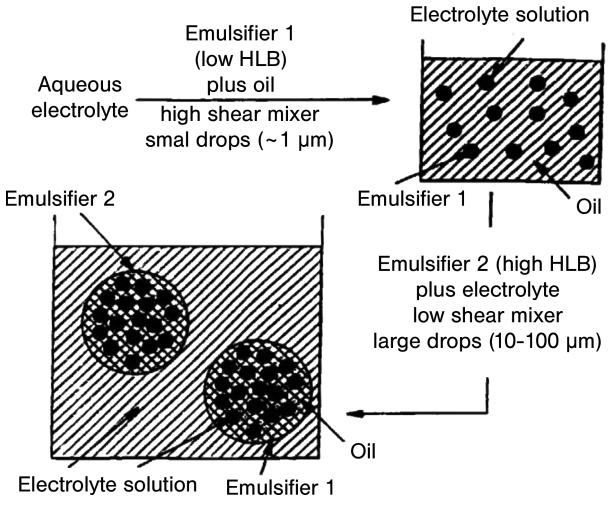

Figure 1.23 Scheme for preparation of W/O/W multiple emulsion.

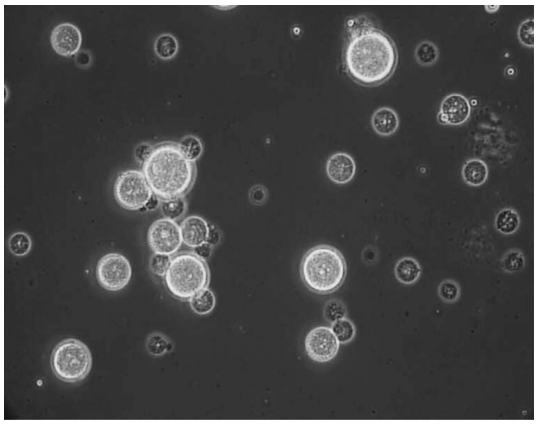

Figure 1.24 Photomicrograph of the W/O/W multiple emulsion.

outside continuous phase. The multiple emulsion was stored at room temperature and 50 °C and photomicrographs were taken at various intervals of time. The multiple emulsion was very stable for several months. A photomicrograph of the W/O/W multiple emulsion is shown in Figure 1.24.

An O/W/O multiple emulsion was made by first preparing a nanoemulsion using INUTEC SP1. The nanoemulsion was then emulsified into an oil solution of Arlacel P135 using a low-speed stirrer. The O/W/O multiple emulsion was stored at room temperature and 50 °C and photomicrographs were taken at various intervals of time. The O/W/O multiple emulsion was stable for several months both at room temperature and 50 °C. A photomicrograph of the O/W/O multiple emulsion is shown in Figure 1.25.

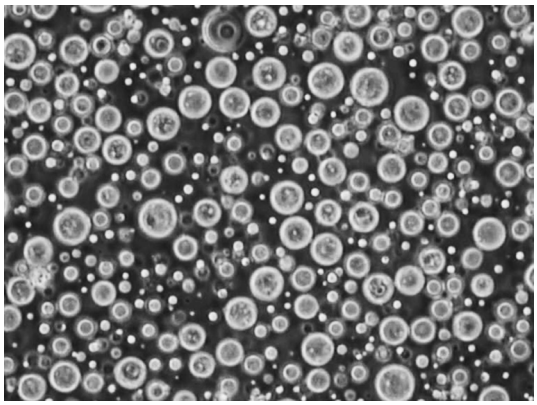

Figure 1.25 Photomicrograph of the O/W/O multiple emulsion.

1.9
Polymeric Surfactants for Stabilization of Liposomes and Vesicles

Liposomes are multilamellar structures consisting of several bilayers of lipids (several μm). They are produced by simply shaking an aqueous solutions of phospholipids, e.g. egg lecithin. When sonicated, these multilayer structures produce unilamellar structures (with a size range of 25–50 nm) that are referred to as liposomes. A schematic diagram of liposomes and vesicles is given in Figure 1.26. Glycerol-containing phospholipids are used for the preparation of liposomes and vesicles: phosphatidylcholine, phosphatidylserine, phosphatidylethanolamine, phosphatidylanisitol, phosphatidylglycerol, phosphatidic acid and cholesterol. In most preparations, a mixture of lipids is used to obtain the optimum structure.

The free energy for an amphiphile in a spherical vesicle of outer and inner radii R_1 and R_2 depends on (1) γ, the interfacial tension between hydrocarbon and water; (2) n_1, n_2, the number of molecules in the outer an inner layers; (3) e, the charge on the polar head group; (4) D, the thickness of the head group; and (5) v, the hydrocarbon volume per amphiphile (taken to be constant) [31].

The minimum free energy, ${\mu_N}^0$, configuration per amphiphile for a particular aggregation number N is given by [31]

$$ {\mu_N}^0(\min) = 2a_0\gamma\left(1 - \frac{2\pi Dt}{Na_0}\right) \tag{22} $$

where a_0 is the surface area per amphiphile in a planer bilayer ($N = \infty$).

Several conclusions can be drawn from the thermodynamic analysis of vesicle formation: (1) ${\mu_N}^0$ is slightly lower than ${\mu_N}^0(\min)$ ($= 2a_0\gamma$); (2) since a spherical vesicles has much lower aggregation number N than a planer bilayer, then spherical vesicles are more favored over planer bilayers; (3) $a_1 < a_0 < a_2$; (4) for vesicles with a radius $> R_1{}^c$, there are no packing constraints – these vesicles are not favored over smaller vesicles which have lower N; (5) the vesicle size distribution is nearly Gaussian, with a narrow range; for example, vesicles produced from phospatidylcholine (egg lecithin) have $R_1 \approx 10.5 \pm 0.4$ nm – the maximum hydrocarbon chain length is ~1.75 nm; (6) once formed, vesicles are homogeneous

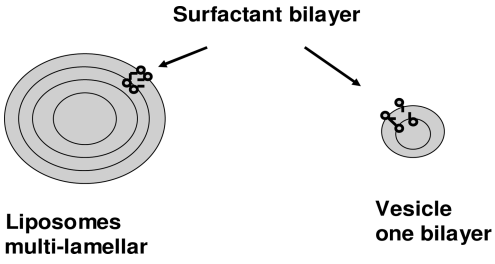

Figure 1.26 Schematic representation of liposomes and vesicles.

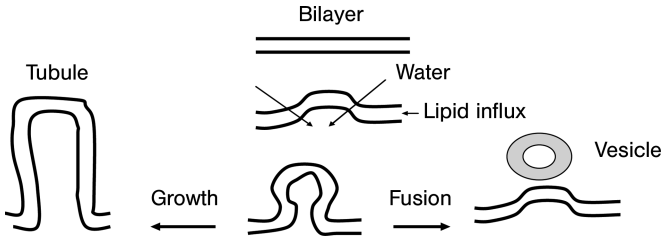

Figure 1.27 Mechanism of spontaneous formation of a vesicle from a bilayer.

and stable and they are not affected by the length of time and strength of sonication; and (7) sonication is necessary in most cases to break up the lipid bilayers which are first produced when the phospholipid is dispersed into water.

A schematic representation of the formation of bilayers and their break-up into vesicles is shown in Figure 1.27.

Liposomes and vesicles are ideal systems for cosmetic applications. They offer a convenient method for solubilizing nonpolar active substances in the hydrocarbon core of the bilayer. Polar substances can also be intercalated in the aqueous layer between the bilayer. They will also form lamellar liquid crystalline phases and they do not disrupt the stratum corneum. No facilitated transdermal transport is possible, thus eliminating skin irritation. Phospholipid liposomes can be used as *in vitro* indicators for studying skin irritation by surfactants.

The main problem with liposomes and vesicles is their physical instability on storage. Polymeric surfactants of the A–B–A block type (such as Pluronics PEO–PPO–PEO) can be used to stabilize the liposomes and vesicles [32]. The PPO chain becomes incorporated in the hydrocarbon bilayer, leaving the PEO chain in the aqueous internal and external phases, thus providing steric stabilization. The graft copolymer of INUTEC SP1 can also be used to stabilize the liposomes and vesicles. The alkyl chains are incorporated in the hydrocarbon bilayers leaving polyfructose loops in the aqueous internal and external phases. This provides an effective steric barrier and hence the long-term stability of the liposomes and

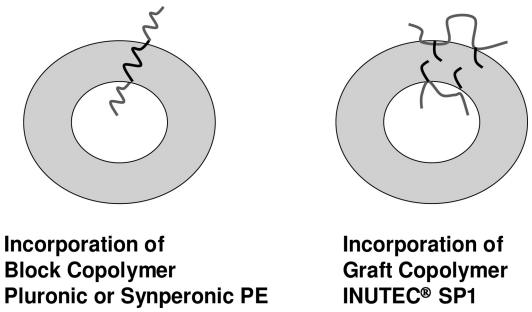

Figure 1.28 Incorporation of block and graft copolymers into the vesicle bilayer.

vesicles can be maintained. In addition, the rigidity of the lipid–polymer bilayer is greatly increased and this prevents the breakdown of the liposomes and vesicles into lamellar structures. A schematic representation of the incorporation of the A–B–A block copolymer (Pluronic or Synperonic PE) into the vesicle structure is given in Figure 1.28. The same figure also shows the incorporation of the graft copolymer INUTEC SP1 into the vesicle bilayer.

1.10 Conclusions

For optimum formulation of cosmetic preparations, one needs to apply the colloid and interface principles. Three main stabilization mechanisms can be identified: electrostatic, steric and electrosteric. The physical states of suspensions and emulsions can be described in terms of the interaction forces between the particles or droplets. Most cosmetic formulation contain self-assembled structures or liquid crystalline phases. The most useful type of liquid crystals is the lamellar phase, which provides an effective barrier against coalescence of the emulsions. These lamellar liquid crystalline structures can enhance penetration of lipophilic and hydrophilic active ingredients. They also provide effective and prolonged moisturization. Polymeric surfactants provide effective stabilization against flocculation and coalescence. They also reduce Ostwald ripening in nanoemulsions. Polymeric surfactants are also applied for stabilization of multiple emulsions of both the W/O/W and O/W/O types. Polymeric surfactants are also used for the stabilization of liposomes and vesicles. The above benefits of polymeric surfactants justify their application in cosmetic preparations. Apart from their excellent stabilization effect, they also eliminate any skin irritation.

References

1 M.M. Breuer, in *Encyclopedia of Emulsion Technology*, Vol. 2, Chap. 7, P. Becher (ed.), Marcel Dekker, New York, 1985.
2 S. Harry, in *Cosmeticology*, J.B. Wilkinson, R.J. Moore (eds.), Chemical Publishing, New York, 1981.
3 S.E. Friberg, *J. Soc. Cosmet. Chem.*, **41**, 155 (1990).
4 A.M. Kligman, in *Biology of the Stratum Corneum in Epidermis*, W. Montagna (ed.), Academic Press, New York, 1964, pp. 421–446.
5 P.M. Elias, B.E. Brown, P.T. Fritsch, R.J. Gorke, G.M. Goay, R.J. White, *J. Invest. Dermatol.*, **73**, 339 (1979).
6 S.E. Friberg, D.W. Osborne, *J. Dispers. Sci. Technol.*, **6**, 485 (1985).
7 S.C. Vick, *Soaps Cosmet. Chem. Spec.*, 36 (1984).
8 Th. Tadros, *Applied Surfactants*, Wiley-VCH, Weinheim, 2005.
9 J. Lyklema, Structure of the solid/liquid interface and the electrical double layer, in *Solid/Liquid Dispersions*, Th.F. Tadros (ed.), Academic Press, London, 1987.
10 B.H. Bijesterbosch, Stability of solid/liquid dispersions, in *Solid/Liquid Dispersions*, Th.F. Tadros (ed.), Academic Press, London, 1987.
11 Th.F. Tadros, Polymer adsorption and dispersion stability, in *The Effect of Polymers on Dispersion Properties*, Th.F. Tadros (ed.), Academic Press, London, 1981.

12 D.H. Napper, *Polymeric Stabilization of Colloidal Dispersions*, Academic Press, London, 1983.
13 P.J. Flory, W.R. Krigbaum, *J. Chem. Phys.*, **18**, 1086 (1950).
14 E.W. Fischer, *Kolloid Z.*, **160**, 120 (1958).
15 E.L. Mackor, J.H. van der Waals, *J. Colloid Sci.*, **7**, 535 (1951).
16 H.R. Kruyt (ed.), *Colloid Science*, Vol. I, Elsevier, Amsterdam, 1952.
17 E.J.W. Verwey, J.Th.G. Overbeek, *Theory of Stability of Lyophobic Colloids*, Elsevier, Amsterdam, 1948.
18 F.Th. Hesselink, A. Vrij, J.Th.G. Overbeek, *J. Phys. Chem.*, **75**, 2094 (1971).
19 K. Holmberg, B. Jonsson, B. Kronberg, B. Lindman, *Surfactants and Polymers in Aqueous Solution*, Wiley, New York, 2003.
20 R.G. Laughlin, *The Aqueous Phase Behavior of Surfactants*, Academic Press, London (1994).
21 K. Fontell, *Mol. Cryst. Liquid Cryst.*, **63**, 59 (1981).
22 K. Fontell, C. Fox, E. Hanson, *Mol. Cryst. Liquid Cryst.*, **1**, 9 (1985).
23 D.F. Evans, H. Wennerstrom, *The Colloid Domain, Where Physics, Chemistry and Biology Meet*, Wiley, New York, 1994.
24 Th.F. Tadros, A. Vandamme, B. Levecke, K. Booten, C.V. Stevens, *Adv. Colloid Interface Sci.*, **108–109**, 207 (2004).
25 D. Exerowa, G. Gotchev, Kolarov, Khr. Khristov, B. Levecke, Th. Tadros, *Langmuir*, **23**, 1711 (2007).
26 D. Exerowa, P.M. Kruglyakov, *Foam and Foam Films*, Elsevier, Amsterdam, 1998.
27 J. Nestor, J. Esquena, C. Solans, P.F. Luckham, M. Musoke, B. Levecke, K. Booten, Th.F. Tadros, *J. Colloid Interface Sci.*, **311**, 430 (2007).
28 Tharwat Tadros, P. Izquierdo, J. Esquena, C. Solans, *Adv. Colloid Interface Sci.*, **108–109**, 303 (2004).
29 D. Attwood, A.T. Florence, *Surfactant Systems,Their Chemistry, Pharmacy and Biology*, Chapman and Hall, New York, 1983.
30 J.L. Grossierd, M. Seiller (eds.), *Multiple Emulsions: Structure, Properties and Application*, Editions de Santé, Paris, 1997.
31 J.N. Isrealachvili, D.J. Mitchell, B.W. Ninham, *J. Chem. Soc., Faraday Trans. 2*, **72**, 1525 (1976).
32 K. Kostarelos, Th.F. Tadros, P.F. Luckham, *Langmuir*, **15**, 369 (1999).